40

Lea Žibret, Martina Cvetković, Maruša Borštnar, Mojca Loncnar, Andrej Ipavec and Sabina Dolenec

Use of steel slag for the synthesis of belite sulfoaluminate clinker

USE OF STEEL SLAG FOR THE SYNTHESIS OF BELITE-SULFOALUMINATE CLINKER

L. Žibret[1], M. Cvetković[1], M. Borštnar[1], M. Loncnar[2], A. Ipavec[3] and S. Dolenec[1]

[1] Slovenian National Building and Civil Engineering Institute, Department of Materials, Laboratory for Cements, Mortars and Ceramics
Dimičeva ulica 12, SI-1000 Ljubljana, Slovenia, EU
e-mail: lea.zibret@zag.si, martina_cvetkovic@yahoo.com, marusa.borstnar@zag.si, sabina.dolenec@zag.si

[2] SIJ Acroni d.o.o.
Cesta Borisa Kidriča 44, SI-4270 Jesenice, Slovenia, EU
e-mail: mojca.loncnar@acroni.si

[3] Salonit Anhovo d.d.
Anhovo 1, SI-5210 Deskle, Slovenia, EU
e-mail: andrej.ipavec@salonit.si

SUMMARY: Belite-sulfoaluminate (BCSA) cements are low-carbon mineral binders, which require low energy consumption and allow the incorporation of various secondary raw materials in the clinker raw meal. In this study two types of unprocessed steel slags, coming from stainless steel production, were incorporated in the BCSA clinkers. The clinker phase composition, clinker reactivity, and the compressive strength of the cement were studied to evaluate the possible use of the slag in BCSA clinkers. The cement clinkers were synthesized by using natural raw materials, white titanogypsum, mill scale, as well as two different steel slags: (i) EAF S slag, which is a by-product of melting the recycled steel scrap in an electric arc furnace, and (ii) ladle slag as a by-product of the processes of secondary metallurgy, in various quantities. Raw mixtures with two different targeted phase compositions varying in belite, calcium sulfoaluminate and ferrite phases were sintered at 1250 °C. Clinker phases were determined by Rietveld quantitative phase analysis, while their distribution, morphology and incorporation of foreign ions in the phases were studied by SEM/EDS analysis. The clinker reactivity was determined by isothermal calorimetry. BCSA cements were prepared by adding titanogypsum. The compressive strength of the cement pastes was determined after 7 days of hydration. The presence of a predicted major clinker phases was confirmed by Rietveld analysis, however periclase was also detected. Microscopy revealed subhedral grains of belite and euhedral grains of calcium sulfoaluminate phases, while ferrite occurred as an interstitial phase. The results showed differences in the microstructure and reactivity of the clinker and cement, which can be attributed to varying amounts of ettringite due to different slag types.

KEY WORDS: belite-sulfoaluminate cement, cement clinker, steel slags, clinker microstructure, cement reactivity

1 INTRODUCTION

Today one of the main issues is a reduction of the carbon footprint, which is being implemented in various fields. In construction materials it can be solved by development of new low-carbon mineral binders, like belite-sulfoaluminate (BCSA) cements, also known as belite-ye'elimite-ferrite (BYF) cements [1-3]. One of the main issues for the production of such cement is to obtain a sufficient source of aluminium [2]. Since the natural source of Al, bauxite, is too expensive and also geographically-limited, many studies are focused on its replacement by Al-rich secondary raw materials [4-6]. However, steel slag can also be incorporated in BCSA clinkers [7].

This study is focused on the use of two types of steel slags for the production BCSA clinker – electric arc furnace slag from stainless steel production (EAF S) and ladle slag as a by-product of the processes of secondary metallurgy. BCSA clinkers of the two targeted compositions were prepared and phase composition was determined for clinkers, using two different raw mixtures. Further microstructural investigations, clinker reactivity and compressive strength after 7 days of curing were performed for clinkers, sintered at 1250 °C.

2 MATERIALS

The four clinkers having two nominal phase compositions: 65 wt% C_2S, 20 wt% $C_4A_3\acute{S}$, 10 wt% C_4AF or 50 wt% C_2S, 35 wt% $C_4A_3\acute{S}$, 10 wt% C_4AF (Table 1), were prepared with proportion of limestone, flysch, white titanogypsum and with either EAF S slag, which is generated during stainless-steel production in an electric arc furnace or ladle slag as a by-product of the processes of secondary metallurgy (AOD and VOD reactor) for an aluminium source. Sampling of slag generated during the production of selected stainless-steel grades, two coming from austenitic stainless CrNi steel and one from austenitic stainless CrNiMo steel were made. Two representative samples were prepared by mixing the sampled slag from three equivalent parts. Unprocessed slag was used. However, the metal phases were removed by sieving and magnets before grinding the slag for the chemical analysis and synthesis of the clinkers in the laboratory.

Bauxite, calcite powder and mill scale were also used for correction. Materials were proportioned by adapting the Bogue method [8]. Raw mix proportioning is given in table 3. The chemical composition of raw materials is given in Table 2. It was determined by wet chemistry methods according to EN 196-2 [9] and X-ray fluorescence spectroscopy (XRF).

Table 1: Targeted phase composition of prepared clinkers (wt%).

	C_2S	$C_4A_3\acute{S}$	C_4AF	Total
KEOP-1	65	20	10	95
KEOP-2	50	35	10	95
KVOD/AOD-1	65	20	10	95
KVOD/AOD-2	50	35	10	95

Table 2: Chemical composition of raw materials (wt%).

	Limestone	Titanogypsum	Bauxite	Flysch	Calcite	Mill scale	EAF S slag	Ladle slag
LOI 950°C	41.41	21.35	0.15	24.65	42.80	0.00	0.00	0.00
*SiO_2	4.76	0.13	5.88	32.02	n.a.	1.08	24.62	24.43
*Al_2O_3	0.86	1.16	87.69	7.74	n.a.	0.20	7.18	6.79
*Fe_2O_3	0.51	0.04	1.89	3.49	n.a.	95.75	2.03	1.75
*CaO	51.51	32.62	0.06	28.83	56.06	0.19	48.06	53.70
*MgO	0.90	0.04	0.52	1.69	n.a.	0.29	10.30	9.40
*SO_3	0.09	45.39	0.17	0.07	n.a.	0.01	b.d.l.	b.d.l.
**Na_2O	0.81	0.26	0.08	0.54	n.a.	0.67	b.d.l.	b.d.l.
**K_2O	0.14	0.01	0.39	1.33	n.a.	0.02	b.d.l.	b.d.l.
**TiO_2	0.04	0.72	3.81	0.38	n.a.	0.01	0.99	0.63
**Cr_2O_3	0.02	0.02	0.07	0.02	n.a.	0.08	2.68	1.05
**MnO	0.04	0.01	0.01	0.07	n.a.	0.60	1.70	0.72
**NiO	b.d.l.	b.d.l.	b.d.l.	0.01	n.a.	0.12	0.05	0.05

* - EN 196-2 [9]; ** - XRF; b.d.l. – below the limit of detection; n.a. – not analyzed

Table 3: Raw mix design (wt%).

Raw mix	Limestone	Titanogypsum	Bauxite	Flysch	Calcite	Mill scale	EAF S slag	Ladle slag
KEOP-1	37.6	4.1	5.6	33.1	3.6	0.7	15.3	-
KEOP-2	39.8	7.4	13.3	22.7	3.4	1.0	12.4	-
KVOD/AOD-1	35.6	4.2	5.6	33.3	3.4	0.7	-	17.2
KVOD/AOD-2	36.0	7.6	13.7	19.8	3.2	1.1	-	18.6

All raw materials were homogenized and ground to pass through a 200 μm sieve. Raw mixtures (200 g) were homogenized for 3 h in 200 ml of isopropanol. Pressed pellets were prepared using a HPM 25/5 press at 10.6 kN. For each pellet 15 g of material was used. The clinker mixtures were subjected to a uniform heating regime: a heating rate of 10 °C/min, holding time 1 hour at a sintering temperature of 1250 °C, and natural cooling in a closed furnace. Furthermore, after sintering all the clinkers were ground to a particle size bellow 125 μm and the cement was prepared by adding 20.3 wt% of white titanogypsum. The amount of gypsum needed was calculated according to [8].

3 METHODS

The phase composition of the clinkers was determined using an X-ray diffraction in a PANalytical Empyrean X-ray diffractometer equipped with CuKα radiation with λ = 1.54 A. The samples were milled to a particle size of less than 63 μm. The ground powder was manually back-loaded into a circular sample holder (diameter 16 mm) to mitigate the preferred orientation effect for XRD data collection. The data were collected at 45 kV and a current of 40 mA, over the 2θ range from 4° to 70°, at a scan rate of 0.026° 2θ/min. The obtained data were analysed using X'PertHighScore Plus diffraction software from PANalytical, using PAN-ICSD V3.4 powder diffraction files. All Rietveld refinements were done using X'Pert High Score Plus diffraction software from PANalytical, using the structures for the phases from ICDD PDF-4+ 2016 RDB powder diffraction files. The following codes have been used: β C_2S (04 007 2687), γ C_2S (04 010 9508), $C_4A_3Ś$ orthorhombic (04 011 1786), $C_4A_3Ś$ cubic (04 009 7268), C_4AF (04 006 8923, 98 026 1869), M (01 071 1176). The amorphous phase was not considered.

The cross-sections of the selected clinker samples (KEOP-1, KVOD/AOD-1) were examined using a JEOL IT5500 Scanning Electron Microscope (SEM) equipped with an Energy Dispersive X-ray spectrometer (EDS), at an accelerating voltage of 20 kV, and a working distance of 10 mm.

The reactivity of clinkers from the selected phase composition for two types of slags (KEOP-1, KVOD/AOD-1) was assessed by isothermal conduction calorimetry using a TAM Air calorimeter (TA Instruments). The mixtures (w/c 0.4) were hand mixed for 5 min and then placed into the calorimeter. However, external mixing could lead to the loss of some very early hydration data [11]. The heat evolution was evaluated for 3 days at 20 °C.

For the determination of the compressive strength of the selected cements of high belite phase composition, incorporating EAF S and ladle slag (KEOP-1, KVOD/AOD-1), cement pastes with a water/cement (w/c) ratio of 0.4 were cast into prismatic moulds, 10 × 10 × 25 mm. The samples of the cement pastes were demoulded 24 h after casting, and cured until testing in sealed plastic bags under laboratory conditions at T (21 ± 2) °C and 95% RH until testing. The compressive strength was determined after 7 days on three specimens per mixture using ToniNORM, Toni-Technic by Zwick testing machine with a loading rate of 0.04 kN/s.

4 RESULTS AND DISCUSSION

4.1 X-ray powder diffraction

XRD pattern for main clinker phases is shown on Figure 1 and the results of quantitative XRD analysis (Rietveld refinement) are given in Table 4. Besides targeted main clinker phases (Table 1) periclase (M) was detected.

Table 4. Phase composition of the clinkers, obtained by X–ray powder diffraction (wt%).

	β-C_2S	γ-C_2S	$C_4A_3Ś$ cub.	$C_4A_3Ś$ ortor.	C_4AF	M
KEOP-1	65.9	0.2	8.5	12.9	9,7	2,8
KEOP-2	52.6	0.0	17.1	19.8	8,5	2,1
KVOD/AOD-1	66.0	1.5	7.6	11.2	10,3	3,3
KVOD/AOD-2	49.6	0.2	13.2	23.7	10,0	3,4

If we compare the samples according to the type of slag used, clinkers of high belite phase composition that contained EAF S (KEOP-1) slag had higher $C_4A_3Ś$ content than ladle slag clinkers of the same targeted phase composition (KVOD/AOD-1). However, for the low belite phase composition the difference in $C_4A_3Ś$ content due to slag type was not evident. On the other hand, C_2S content does not significantly change due to the type of slag incorporated in the clinker (Table 4). C_4AF content is close to the targeted phase composition in all the samples. Clinkers with ladle slag have more C_4AF than clinkers with EAF slag, although the difference is not very convincing. Periclase according to the added type of slag does not show significant differences (Table 4).

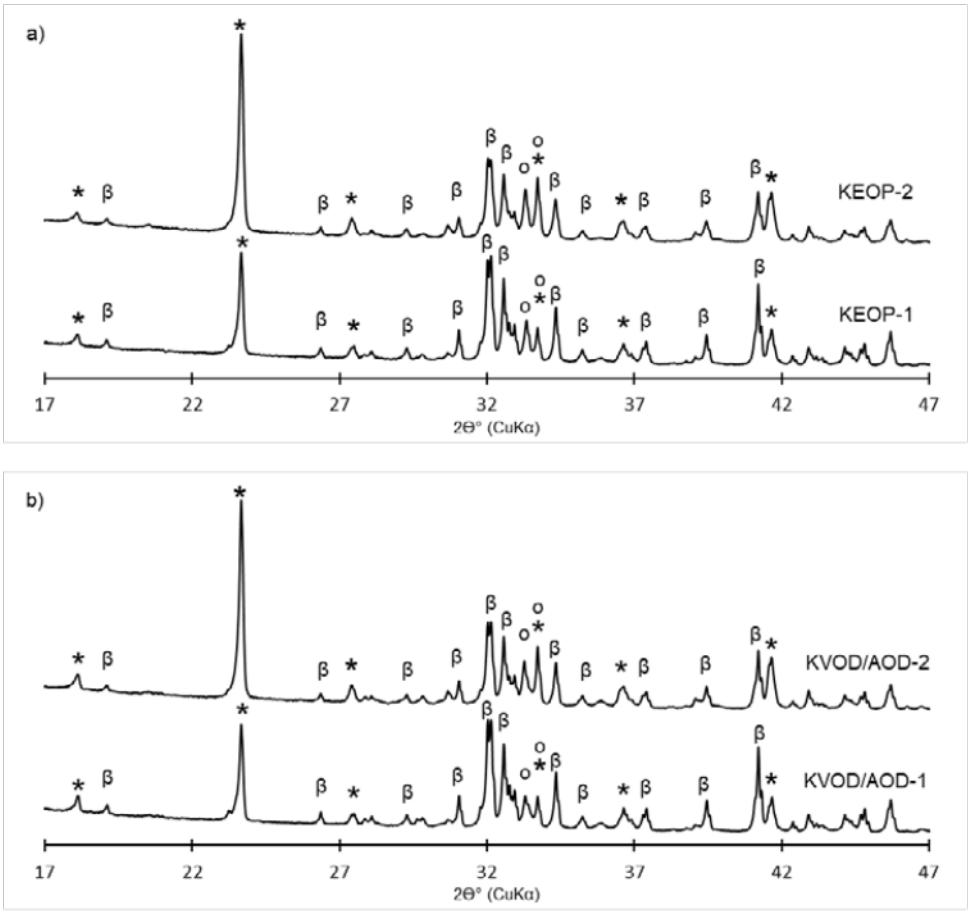

Figure 1: XRD pattern of clinkers with EAF S slag (a) and ladle slag (b). Legend for the targeted clinker phases: * - $C_4A_3Ś$; β - C_2S; o - C_4AF.

4.2 SEM/EDS

SEM/EDS analysis was performed on the selected phase composition (samples KEOP-1 and KVOD/AOD-1). It was carried out in order to check the presence of major and minor phases determined by XRD and to observe the potential microstructural differences regarding the type of slag used. The SEM/BSE images show a similar microstructure for clinkers with EAF S slag (Figure 2a, c) and in clinkers with ladle slag (Figure 1b, d). Belite is presented by subhedral rounded medium grey grains, while calcium sulfoaluminate has a dark grey euhedral hexagonal or quadrilateral crystal cross-sections. The ferrite phase formed an interstitial phase between the calcium sulfoaluminate and belite. Dark euhedral grains of periclase are also evident, which can be attributed to high magnesium content in both slag samples (around 10 wt%). Grain size of the calcium sulfoaluminate, belite and periclase was larger in the clinker with ladle slag (KVOD/AOD-1), where the grain diameter average was 6.7 μm for belite, 4.2 μm for calcium sulfoaluminate and 3.2 μm for periclase. In the clinker with EAF S slag, the grain size average was 5.5 μm for belite, 3.9 μm for calcium sulfoaluminate and 2.2 μm for periclase.

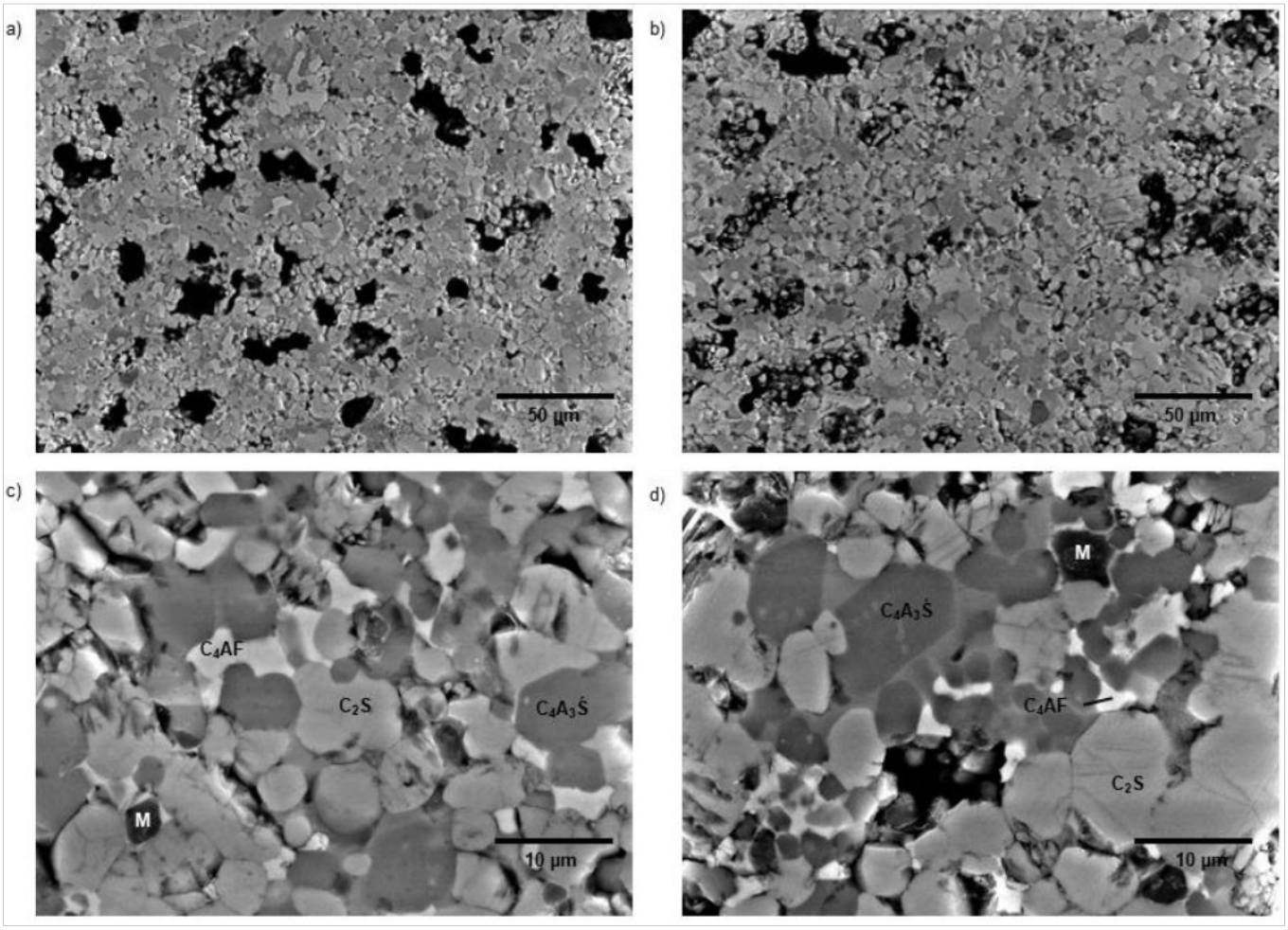

Figure 2: SEM/BSE microphotographs of clinkers KEOP-1 (left) and KVOD/AOD-1 (right).

EDS analysis of the main clinker phases was performed for clinkers of the selected phase composition with EAF S and ladle slag (Figure 2). In clinkers with EAF S slag belite, as well as Ca and Si, it includes the following elements, written in descending order: Al, Mg, Fe, S, K, Na and Ti. In clinkers with the ladle slag the same elements were detected in belite phase, but in a slightly different quantitative order: Al, Fe, Mg, S, Ti, K and Na. Calcium sulfoaluminate in both samples, as well as Ca, Al and S, consisted of Si, Fe, Cr, Mg, K, Na and Ti, while ferrite in both samples, as well as Ca, Al and Fe, it includes Si, Ti, Mn, Mg, S, Cr, K and Na (elements are written in descending order). In periclase, as well as Mg, there was Ca, Si, Al, Fe, Ni, S, K, Ti and Na.

Among the slag derived trace elements, Cr is embedded in calcium sulfoaluminate, Mn and Cr in ferrite and Ni in periclase. The maximum quantities of Ti, which was derived from bauxite, can be found in the ferrite phase (Figure 3).

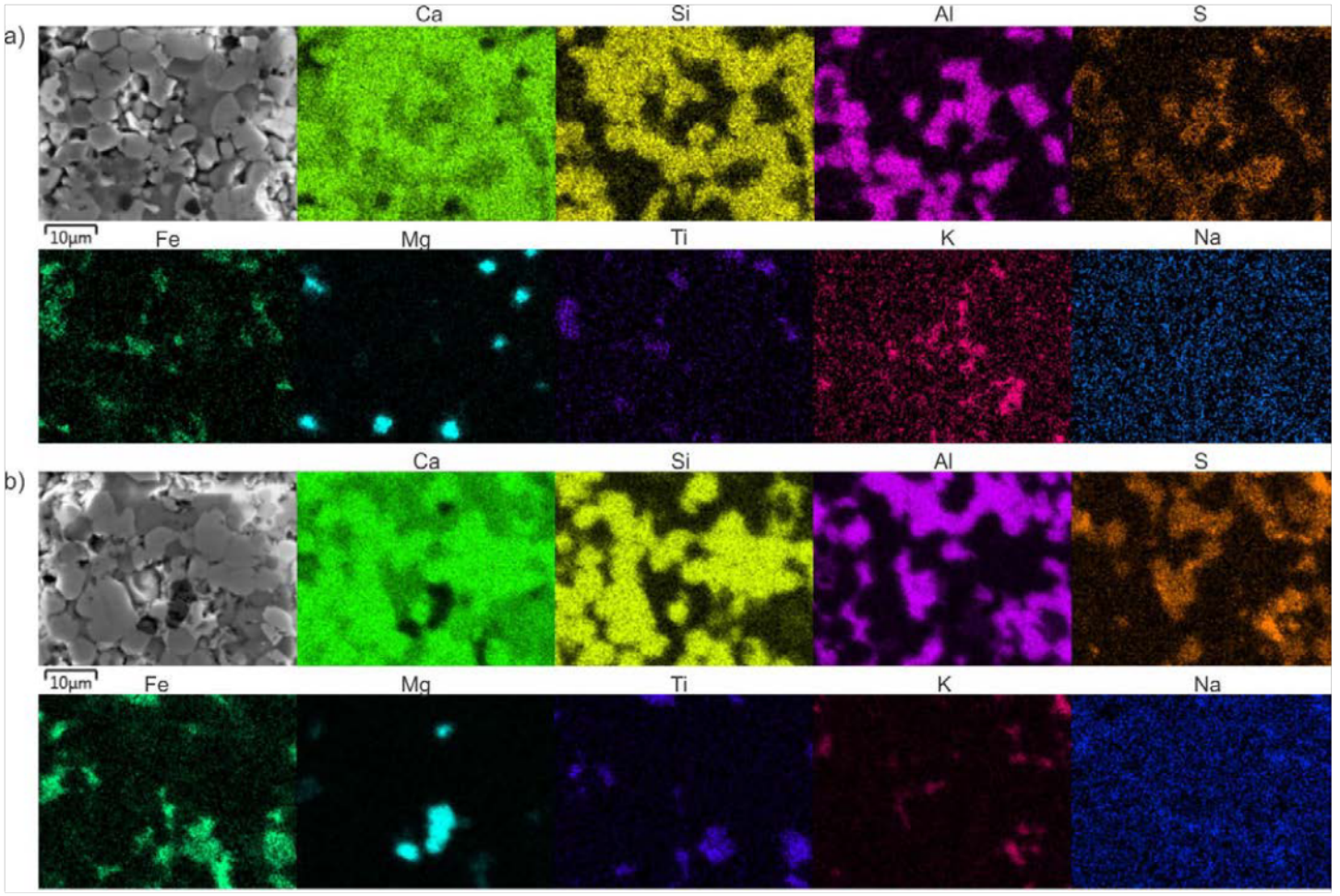

Figure 3: Elemental maps of Ca, Si, Al, S, Fe, Mg, Ti, K and Na for clinkers KEOP-1 (a) and KVOD/AOD-1 (b).

SEM/EDS analysis results in the main part coincided with the results of the XRD analysis. All the main phases whose presence was determined by X-ray powder diffraction were also clearly visible in the SEM/EDS microphotographs of clinkers (belite, ferrite and calcium sulfoaluminate). Among the minor phases, only periclase was clearly evident by SEM/EDS analysis, while other minor phases were not found.

4.3 Isothermal calorimetry

Isothermal calorimetry was performed on clinkers of the selected phase composition with the incorporation of EAF S or ladle slag. There was a significant difference in the calorimetric curves between clinkers with EAF S and ladle slag (Figure 4a, b). The clinker with EAF S slag had one peak during the main hydration phase, which appeared at 18.4 h, with released heat flow of 0.8 mW/g (Figure 4a). Hydration of the clinker with ladle slag starts earlier and has a more complex hydration evolution with two main peaks. The first appears at 6.6 h with a released heat flow of 1.2 mW/g while the second peak appears at 15.9 h with a released heat flow of 1.2 mW/g. According to the literature, the first peak during the main hydration phase can be attributed to ettringite crystallization, while the second peak during the main hydration phase most probably reflects the formation of the monosulfate phase after the complete sulfate depletion in the presence of water [10-14]. Therefore, due to the crystallization of the monosulfate, a reduced amount of ettringite can be expected in the clinker with ladle slag. The difference in the reaction pattern is evident also from the cumulative heat curves (Figure 4b), where the total heat of hydration after 72 h for the EAF S slag clinker is 103.4 J/g and for the ladle slag clinker it is 112.2 J/g.

Differences in the calorimetric pattern of hydration between the EAF S slag clinker and the ladle slag clinker could be attributed to the following factors: (i) increased calcium sulfoaluminate content in the EAF S slag clinker, which may result in more ettringite formation; (ii) increased grain size in the ladle slag clinker, which may decrease clinker reactivity; (iii) variations regarding minor elements, incorporated in main clinker phases.

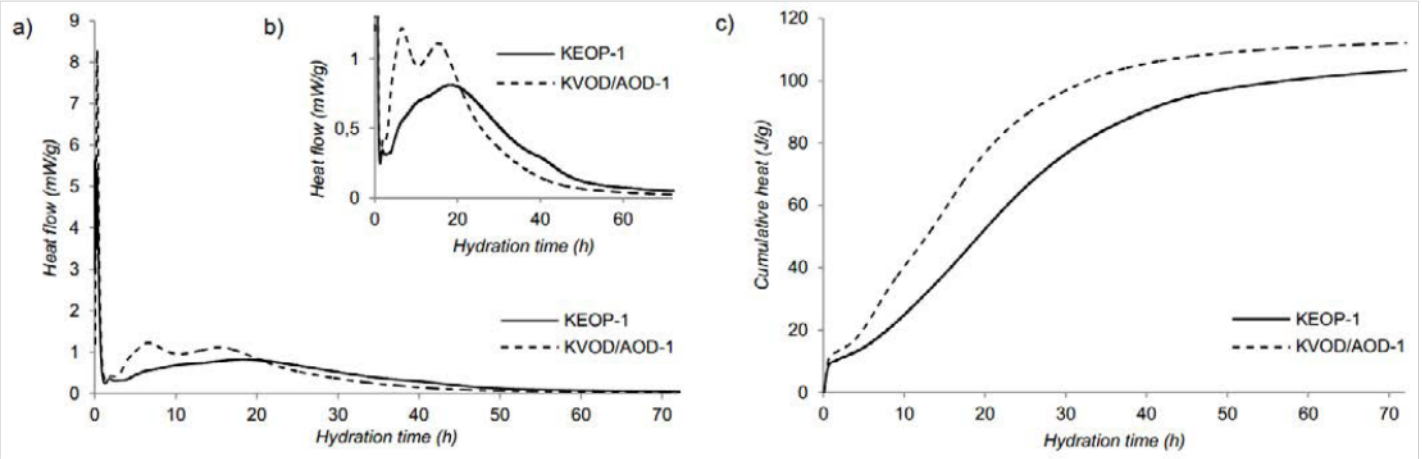

Figure 4: Isothermal conduction calorimetry for clinkers KEOP-1 with addition of EAF S slag and KVOD/AOD-1 with ladle slag: a) heat flow evolution, b) calorimetric curves at main hydration phase and c) cumulative heat evolution.

4.4 Compressive strength

After 7 days of curing clinkers with EOP S slag, it developed a compressive strength of 28.1 N/mm^2, while the clinkers with ladle slag developed a compressive strength of only 22.8 N/mm^2 (Table 5). The lower compressive strength of the clinker with ladle slag can be explained by the reduced amount of ettringite, which leads to a lower volume of hydrates and thus to a lower compressive strength [10].

Table 5: Compressive strength of cement pastes after 7 days of curing.

Sample	KEOP-1	KVOD/AOD-1
Compressive strength (N/mm^2)	28.1	22.8

5 CONCLUSIONS

The present work focused on evaluating the effect of raw material (different slag types: EAF S slag from stainless steel production and ladle slag as a by-product of the processes of secondary metallurgy) on belite-sulfoaluminate clinker microstructure, reactivity and compressive strength of cement pastes after 7 days of hydration.

In BCSA clinkers with EAF S slag and in BCSA clinkers with ladle slag the main clinker phases were generally developed due to the targeted phase composition. However, in clinkers with EAF S slag more calcium sulfoaluminate phase was formed than in clinkers with the same targeted phase composition with ladle slag. A decrease in the ferrite content was detected in all the samples. Among minor phases periclase was documented by XRD and SEM/BSE analysis.

Both clinkers with both types of slags had a similar microstructure, composed of rounded subhedral belite grains and angular euhedral calcium sulfoaluminate, and periclase grains and ferrite as an interstitial phase. The main clinker phases in the ladle slag clinker had a larger grain size than the main clinker phases in the EAF S clinker, which could contribute to the reduction of ladle slag clinker reactivity.

The hydration curve of the clinker with ladle slag points to a faster formation of ettringite than the clinker with EAF S slag, which was followed by monosulfate precipitation. On the other hand, the clinker with EAF S slag had a slower hydration reaction, most probably due to ettringite formation. Consequently, the clinker with EAF S slag had a higher compressive strength than the clinker with ladle slag.

The differences of the hydration pattern due to the type of slag, incorporated in BCSA clinker, could be attributed to the variation of the chemical composition of both slags, consequently influencing the phase composition, clinker microstructure, its reactivity and the compressive strength of the cement pastes. However, further investigations will be focused on the processed slags (mineral product after metal extraction) with a more constant chemical composition.

ACKNOWLEDGMENTS

Project No. C3330-17-529035 "Raziskovalci-2.0-ZAG-529035" was granted by the Ministry of Education, Science and Sport of the Republic of Slovenia. The investment is co-financed by the Republic of Slovenia, Ministry of Education, Science and Sport and the European Regional Development Fund.

REFERENCES

[1] Gartner, E.: Industrially interesting approaches to “low CO2” cements, *Cement and Concrete Research*, 2004, Vol. 34 No. 9, pp. 1489-1498.
[2] Gartner, E. & Sui, T.; Alternative cement clinkers, *Cement and Concrete Research*, 2018, Vol. 114, pp. 27-39.
[3] Damtoft, J.S. et al.: Sustainable development and climate change initiatives, *Cement and Concrete Research,2008, Vol.* 38 No. 9, pp. 115-127.
[4] Ma, B. et al.: Synthesis and characterization of high belite sulfoaluminate cement through rich alumina fly ash and desulfurization gypsum, *Ceramic Silikáty*, 2013, Vol. 57 No.1, pp. 7-13.
[5] Wang, W. et al.: Ex Experimental investigation and modelling of sulfoaluminate cement preparation using desulfurization gypsum and red mud, *Industrial & Engineering Chemistry Research*, 2013, Vol. 52, pp. 1261-1226.
[6] Kramar, S. et al.: Use of fly ash and phosphogypsum for the synthesis of belite-sulfoaluminate clinker, *Materiales de Construcción*, 2019, Vol. 69, No. 333, pp. 1-12.
[7] Iacobescu, R.I. et al.: Synthesis, characterization and properties of calcium ferroaluminate belite cements produced with electric arc furnace steel slag as raw material, *Cement and Concrete Composites*, 2013, Vol. 44, pp. 1-8.
[8] Chen, I.A. & Juenger, M.C.G.: Synthesis and hydration of calcium sulfoaluminate-belite cements with varied phase compositions, Journal of Materials Science, 2011, Vol. 46, pp. 2568-2577.
[9] EN 196-2. Methods of testing cement – Part 2, Chemical analysis of cement, Slovenian Institute for Standardization (SIST) and European Committee for standardization (CEN), 2013, p. 78.
[10] Ben Haha et al.: Advances in understanding ye'elimite-rich cements, *Cement and Concrete Research*, 2019, Vol. 123, pp. 1-20.
[11] Winnefeld, F. & Lothenbach,B.: Hydration of calcium sulfoaluminate cements – experimental findings and thermodynamic modelling, *Cement and Concrete Research*, 2010, Vol. 40, pp. 1239-1247.
[12] Bullerjahn, F. et al.: Hydration reactions and stages of clinker composed mainly of stoichiometric ye'elimite,, *Cement and Concrete Research*, 2019, Vol. 116, pp. 120-133.
[13] Rungchet, A. et al.: Hydration and Physico-mechanical Properties of Blended Calcium Sulfoaluminate-belite Cement Made of Industrial By-products, *KMUTNB International Journal of Applied Science and Technology*, 2016, Vol. 9, No. 4, pp. 279-287.
[14] Winnefeld, F. et al.: Using gypsum to control hydration kinetics of CSA cements, *Construction and Building Materials*, 2017, Vol. 155, pp. 154-163.